Video Article

The *Drosophila* Imaginal Disc Tumor Model: Visualization and Quantification of Gene Expression and Tumor Invasiveness Using Genetic Mosaics

Juliane Mundorf[1], Mirka Uhlirova[1]

[1]Institute for Genetics, Cologne Excellence Cluster on Cellular Stress Responses in Aging-Associated Diseases (CECAD), University of Cologne

Correspondence to: Mirka Uhlirova at mirka.uhlirova@uni-koeln.de

URL: https://www.jove.com/video/54585
DOI: doi:10.3791/54585

Keywords: Cancer Research, Issue 116, *Drosophila*, Eye/antennal imaginal disc, Brain, Clonal analysis, MARCM technique, Cancer, Invasiveness, Dissection, Immunostaining, Confocal microscopy, RNA isolation, Transgenic reporters, Transcriptome profiling, Cancer biology

Date Published: 10/6/2016

Citation: Mundorf, J., Uhlirova, M. The *Drosophila* Imaginal Disc Tumor Model: Visualization and Quantification of Gene Expression and Tumor Invasiveness Using Genetic Mosaics. *J. Vis. Exp.* (116), e54585, doi:10.3791/54585 (2016).

Abstract

Drosophila melanogaster has emerged as a powerful experimental system for functional and mechanistic studies of tumor development and progression in the context of a whole organism. Sophisticated techniques to generate genetic mosaics facilitate induction of visually marked, genetically defined clones surrounded by normal tissue. The clones can be analyzed through diverse molecular, cellular and omics approaches. This study describes how to generate fluorescently labeled clonal tumors of varying malignancy in the eye/antennal imaginal discs (EAD) of *Drosophila* larvae using the Mosaic Analysis with a Repressible Cell Marker (MARCM) technique. It describes procedures how to recover the mosaic EAD and brain from the larvae and how to process them for simultaneous imaging of fluorescent transgenic reporters and antibody staining. To facilitate molecular characterization of the mosaic tissue, we describe a protocol for isolation of total RNA from the EAD. The dissection procedure is suitable to recover EAD and brains from any larval stage. The fixation and staining protocol for imaginal discs works with a number of transgenic reporters and antibodies that recognize *Drosophila* proteins. The protocol for RNA isolation can be applied to various larval organs, whole larvae, and adult flies. Total RNA can be used for profiling of gene expression changes using candidate or genome-wide approaches. Finally, we detail a method for quantifying invasiveness of the clonal tumors. Although this method has limited use, its underlying concept is broadly applicable to other quantitative studies where cognitive bias must be avoided.

Video Link

The video component of this article can be found at https://www.jove.com/video/54585/

Introduction

Cancer represents one of the most genetically heterogeneous group of diseases, whose incidence and mortality is dramatically increasing, particularly among the elderly worldwide. Cancer originates clonally from a tumor-initiating cell that escapes inherent tumor suppressor mechanisms and divides out of control. The gradual accumulation of genetic lesions that cooperatively promote growth, proliferation and motility while inhibiting death and differentiation transforms the initial benign overgrowth into a highly malignant, metastatic and deadly tumor. It has become evident that in addition to genetic alterations, tumor progression requires changes in the surrounding stroma and crosstalk between the tumor and multiple cell types (*e.g.*, fibroblasts, immune and endothelial cells) in its microenvironment. Understanding the molecular principles underlying malignant transformation including tumor-stroma interactions is of great importance for developing prevention and early screening strategies, as well as new and effective treatments to combat cancer metastasis and drug resistance.

The fruit fly *Drosophila melanogaster* has become an attractive system for cancer research [1-4] owing to its fast generation time, remarkable conservation of signaling nodes between flies and humans, limited genetic redundancy and wealth of advanced genetic tools that facilitate manipulation of almost any gene in a temporarily and spatially restricted manner. Genetically defined tumors of varying malignancy can be reproducibly engineered in *Drosophila* by introducing gain- and loss-of-function mutations in a subset of progenitors in an otherwise wild type tissue using the MARCM technique [5]. The MARCM tool combines FLP/FRT (FLP recombinase/FLP Recognition Target)-mediated mitotic recombination [6] with FLP-out [7] and Gal4/UAS (Upstream Activation Sequence) [8] target gene expression systems [9]. With this method expression of any UAS-based transgene, including oncogene or fluorescent protein cDNAs or inverted DNA repeats for dsRNA-induced gene silencing, will be restricted to a clone of cells that have lost a specific genetic locus and a Gal4 repressor due to recombination (**Figure 1A**). Clonal patches marked with green fluorescent (GFP) or red fluorescent proteins (*e.g.,* RFP, DsRed, mCherry) can be easily tracked throughout development, isolated and analyzed. Importantly, their behavior can be directly compared to the adjacent wild type tissue. Thus, questions pertinent to the cell autonomous and non-autonomous effects of genetic lesions can be conveniently studied. Similar to mammals, only clones in which multiple oncogenic lesions are combined become malignant in *Drosophila* and recapitulate key hallmarks of mammalian cancer. They overproliferate, evade apoptosis, induce inflammation, become immortal and invasive, ultimately killing the host [10-17].

Here, we describe a protocol to generate genetically defined clonal tumors in the eye/antennal and brain tissue of *Drosophila* larvae using the MARCM technique. The method relies on a MARCM tester stock which expresses the yeast FLP recombinase under the control of the *eyeless* enhancer (*eyFLP*) [18,19]. In this way, GFP-labeled clones are generated in both peripodial and columnar epithelium of the EAD and

the neuroepithelium of the brain throughout embryonic and larval stages (**Figure 1A, B** and reference [20]). Clones can be easily followed until adulthood as the EAD develops into the adult eye, antenna and head capsule while the neuroepithelium gives rise to neuroblasts that produce differentiated optic lobe neurons.

To facilitate extensive molecular, functional and phenotypic characterization of the mosaic tissue, we describe a protocol for dissection of the EAD and brain from the third instar larvae and outline how to process them for three different applications: (i) detection of transgenic fluorescent reporters and immunostaining, (ii) quantification of tumor invasiveness and (iii) analysis of gene expression changes using a quantitative real-time PCR (qRT-PCR) or a high-throughput mRNA sequencing (mRNA-seq) (**Figure 1C**).

The immunostaining protocol can be used to visualize any protein of interest with a specific antibody. Transgenic fluorescent transcriptional reporters provide convenient and precise spatiotemporal information on the activity of a particular signaling pathway. Cell-lineage specific reporters, on the other hand, reflect qualitative and quantitative changes in cell populations within the mosaic tissue and among tumors of distinct genotypes. Quantification of invasive behavior facilitates the comparison of tumor malignancy between genotypes. Finally, the protocol describing collection and processing of mosaic EAD for RNA isolation is suitable for both small and large-scale downstream applications such as reverse transcription followed by qRT-PCR and genome-wide mRNA-seq, respectively. The qualitative and quantitative data obtained from these assays provide novel insights into the social behavior of clonal tumors. Moreover, they produce a solid foundation for functional studies on the role of individual genes, genetic networks and tumor microenvironment in different stages and aspects of tumorigenesis.

Protocol

NOTE: This work utilizes the *eyFLP1; act>y^{+}>Gal4, UAS-GFP; FRT82B, tub-Gal80* MARCM 82B Green tester line [11]. Crossing the MARCM 82B Green tester virgins to males of strains such as *w; UAS-a; UAS-b^{RNAi}, FRT82B c^{mut}* genotype will yield progeny in which mitotic recombination will occur between the right arms of the 3rd homologous chromosomes. In this way, clones homozygous mutant for gene *c* located distal to the FRT82B site will be generated within the EAD and brain neuroepithelium. These clones will express GFP, transgene *a* and dsRNA for gene *b* (**Figure 1A**). Various eyFLP-MARCM tester lines for recombination on the X, 2L, 2R, 3L and 3R have been established and are available within the fly community.

1. Fly Handling, Crosses, and Staging

1. Expand the appropriate MARCM tester stock at room temperature by populating multiple bottles at the same time. Flip the adults into fresh bottles every 2-3 days so that enough virgins can be collected for subsequent crosses.
   NOTE: When collecting virgins, avoid a prolonged exposure to CO_2 as this compromises female fecundity.
2. Depending on the scale of the experiment, set up fly crosses in vials using at least 10 MARCM tester virgins and 4 males (*e.g.*, for imaging of fluorescent reporters and immunostaining) or in bottles with at least 30 virgins and 10 males (*e.g.*, for RNA isolation and quantification of invasiveness).
3. Raise progeny at 25 °C under a long day 16 hr/8 hr light-dark cycle. Flip parents into new vials/bottles every 24 hr to facilitate reproducible staging of larvae and to prevent overcrowding.
   NOTE: Starting on day 6 after egg laying (AEL), the late third instar control larvae stop feeding, start wandering and enter pupariation. In contrast, the onset of the larval-pupal transition can be delayed or non-existent in larvae with EAD bearing hyperplastic or malignant clonal tumors.

2. Collecting Third Instar Larvae

1. For immunostaining, collect about 20 late third instar larvae (wandering on the wall and those of a comparable body size from the food). Use forceps to gently pick larvae from the vial or bottle and transfer them into an embryo glass dish filled with phosphate-buffered saline (PBS).
   1. For RNA isolation and quantification of invasiveness, collect at least 80 late third instar larvae (wandering on the wall and those of a comparable body size from the food). Use a squirt bottle to squirt PBS into a fly bottle containing larvae until the surface is covered.
   2. Soften the top layers of food with a spatula and pour the food mash containing larvae into a Petri dish. Using forceps, gently pick larvae and transfer them into an embryo glass dish filled with PBS.
2. Wash larvae with PBS until all residual food is removed. Inspect the larvae under the fluorescent stereomicroscope with 8 to 16X magnification to discard all "leopard larvae" that carry random GFP-positive spots throughout the larval body (**Figure 2A**, **2B** and see **Discussion Section**).
   NOTE: For RNA isolation include a penultimate washing step in 70% EtOH for 1 min.
3. Place the dish containing selected larvae in PBS on ice until dissection. Process larvae within 30 min to avoid adverse effects of cold and starvation.

3. Dissection of Larvae

1. To dissect the EAD under a stereomicroscope, use one pair of forceps to gently press the middle part of the larva against the glass dish bottom. With the second forceps, grab the larval mouth hooks and pull them away from the body (**Figure 2C**).
   NOTE: The pulling force is often sufficient to break the optic stalks connecting the EAD pair to the brain lobes. If the brain or its parts stay attached to EAD and their presence is not desired for further applications, cut the optic stalks with a help of the two pairs of forceps. For invasive tumors (*e.g.*, *ras^{V12}scrib^{1}*) the connection between EAD and the brain lobes becomes increasingly obscured with time by overgrowing and migrating clonal cells.
   1. To prepare the EAD/brain complex with an intact ventral nerve cord (VNC) (**Figure 2D**), use forceps to cut a larva in the middle of the body. Discard the posterior half.

2. Hold the anterior half of the larval body between the tips of one forceps, flip the larva inside-out by pushing in the mouth hooks with the tip of the second forceps and by rolling the cuticle over it with the first forceps pair.

2. Using forceps carefully remove all extraneous tissues (*e.g.,* salivary glands, fat body, and gut) while leaving the EAD pair or the EAD/brain complex connected to the mouth hooks. Disentangle the mouth hooks from the overlying cuticle. Free the VNC by severing the axonal projections extending to body muscles and epidermis (**Figures 1B, 2C, 2D**).
   NOTE: The mouth hooks allow for safe manipulation of tissue with forceps and facilitate more efficient sinking and easy recognition of tissue during washing. Dissected EAD change morphology relatively fast when kept unfixed in PBS. Limit the dissection time to 20-30 min.
3. To transfer the tissue, coat a P20 micropipette tip by pipetting the remaining body carcasses several times up and down. To transfer the larger EAD/brain complexes, cut the P20 micropipette tip with scissors.
   NOTE: The coating procedure is critical to prevent sticking and loss of dissected tissue during transfer. Use of a P20 micropipette minimizes the transfer of PBS into fixative solution, limiting unwanted dilution.
   1. For immunostaining, transfer the dissected EAD into a 0.5 ml tube filled with 400 µl 4% paraformaldehyde (PFA) fixative. Use 1.5 ml tube with 1 ml PFA for larger EAD/brain complexes meant for scoring of invasiveness.
      CAUTION: PFA is highly toxic. Wear protective gloves and clothing. Avoid contact with skin, eyes or mucous membranes.
   2. For RNA isolation transfer the dissected EAD into a new glass dish filled with cold PBS. Use forceps to clean EAD from the ring and lymph glands, to minimize sample contaminations.
   3. Detach the EAD from the mouth hooks by severing the connection between the antenna discs and mouth hooks using forceps (**Figure 2E**). To avoid RNA degradation and gene expression artifacts, limit the dissection time to 30 min. Proceed to step 7.
      NOTE: An experienced researcher can dissect about 60 larvae in 30 min excluding time needed for larvae collection and washing. Total RNA yields depend on the EAD size that vary among genotypes and developmental stages. Dissection of 80-100 control EAD pairs from late third instar larvae should yield 5-8 µg total RNA.

4. Fixing, Immunostaining, and Mounting

1. Fix samples in PFA fixative for 25 min while nutating at room temperature. The fixation time can be extended up to 60 min without altering tissue morphology and the antigenicity of proteins.
2. Remove the fixative and wash samples with PBST (PBS with 0.1% Triton X-100) three times for 10 min using a nutator. Use sufficient volume of PBST for each washing step (400 µl/0.5 ml tube).
   NOTE: Fixed EAD/brain complexes meant for scoring of invasiveness do not require immunostaining. GFP signal remains well visible after fixation. Proceed to step 4.4 for the final dissection.
   1. For immunostaining, block tissue in 200 µl of a blocking solution (PBST with 0.3% BSA) for 20 min with gentle agitation at room temperature.
      1. Incubate with primary antibodies diluted in 100 µl of a blocking solution overnight at 4 °C while gently shaking. Refer to primary antibody datasheet or published literature for recommended antibody dilution.
         NOTE: The primary antibody dilution might need to be optimized.
      2. Following five 10 min washes in PBST, stain tissue with the fluorescent secondary antibodies diluted in blocking solution while gently shaking for 2 hr at room temperature or overnight at 4 °C in the dark.
      3. Wash samples three times 10 min in PBST.

3. Replace PBST with 500 µl of DAPI-staining solution. To label F-actin, add phalloidin conjugated to a fluorescent dye to DAPI-staining solution. After 15 min nutation in the dark, wash tissue once for 10 min with PBST.
   NOTE: F-actin labeling can be carried out independently of DAPI staining.
4. For the final dissection step, transfer tissue back into a PBS-filled glass dish using a 1 ml pipette. Using the two pairs of forceps clip off the mouth hooks.
   1. Separate the brains that will be used for quantification of invasiveness from the EAD by cutting the optic stalk as overgrown EAD might hamper the analysis.

5. Place a drop of the mounting medium (15 µl for a 22 mm x 22 mm coverslip) on an objective slide. With the help of forceps tips, distribute the medium into a thin layer. Transfer EAD, brains or the EAD/brain complexes into the mounting medium with a P20 micropipette.
6. Use the forceps tips or a tungsten rod to distribute tissue and straighten the VNC on the slide.
7. To avoid formation of bubbles while mounting, first touch one edge of a coverslip to the mounting medium and then slowly lower onto the mounting medium with the help of forceps. Use small pieces of filter paper or tissue wipe to absorb excess mounting medium around the coverslip edges.
   NOTE: DABCO/Poly(vinyl alcohol) 4-88 mounting medium hardens at 4 °C within an hour. Slides can be stored for months at 4 °C.

5. Confocal Imaging

1. Acquire single confocal sections and stacks using a confocal microscope equipped with 20X, 40X and 60X oil objectives.
2. Prevent pixel saturation. Use same image acquisition parameters including image resolution, laser input power, gain, offset, frame averaging, a step size in a z-series and maintain these settings for all genotypes to allow for comparisons of pixel intensities between different genotypes [21,22].
   NOTE: For visualization of EAD/brain complex, generate maximum projections and stitch respective, neighboring images. For final image preparation, use post image processing software for panel assembly and to adjust brightness and contrast.

6. Quantification of Tumor Invasiveness

1. Define a scoring system that will characterize the different levels of tumor invasiveness considering the spatial pattern of invasion and the amount of GFP-positive cells spreading into the brain and VNC. Prepare evaluation sheets for documentation (**Figure 3A**).
2. Mount at least 80 fixed intact brains for each genotype on one slide using 40 µl of the mounting medium per 24 mm x 50 mm coverslip.
    1. To allow unbiased scoring, ask a neutral party to anonymize the slides, so that the scoring procedure is unbiased. Evaluate anonymized slides by two lab members independently. Disclose genotypes only after the counting is finished.
3. Evaluate the degree of malignancy by a blind scoring of mounted brains under a fluorescent stereomicroscope equipped with a GFP filter set. Use a marker to label brains that have been already viewed to avoid double counting (**Figure 3B**).
4. Calculate the percentage of brains falling into each of the defined invasive categories per genotype. Determine the statistical significance using a chi-square test (**Figure 3C**).

7. RNA Isolation, DNase Treatment, and Quality Check

NOTE: All reagents (solutions, plasticware) used in the following steps should be free of RNase activity. Always wear gloves and use a chemical hood for work with organic solvents.

1. Transfer the clean EAD with a coated P20 micropipette tip into 1.5 ml tube.
2. Let tissue sink to the bottom of the tube, carefully remove PBS and replace it with 100 µl RNA lysis reagent (sufficient for up to 140 EAD).
3. Lyse tissue by vortexing. At this point, samples can be deep frozen in liquid nitrogen and stored at -80 °C or directly processed with a standard RNA isolation protocol.
   NOTE: Samples of similar genotypes from multiple dissection rounds can be pooled once in RNA lysis reagent.
4. Fill the sample volume to 0.9 ml with RNA lysis reagent. Add 0.2 ml of chloroform and mix samples vigorously for 15-20 sec.
5. Following 2 to 3 min incubation at room temperature, centrifuge the samples at 10,000 x g for 15 min at 4 °C.
6. Transfer colorless upper aqueous phase containing RNA into a fresh tube without disturbing the interphase. Stay away from the interphase as it contains proteins and genomic DNA.
   NOTE: The recovered volume should be about 60% of the volume of RNA lysis reagent used for homogenization.
7. Precipitate the RNA by adding 0.5 ml of isopropyl alcohol. Vortex and incubate samples at room temperature for 10 min.
8. Centrifuge the samples at 10,000 x g for 15 min at 4 °C.
9. Discard the supernatant and wash the RNA pellet once with 600 µl of 75% ethanol. After a short vortex and centrifugation (10,000 x g for 7 min at 4 °C) discard all ethanol and let the RNA pellet air-dry for 5-10 min placing the open tube on a clean tissue wipe.
   NOTE: The RNA pellet might be visible as a tiny opaque/white stripe at the bottom of the tube or invisible. The remaining ethanol drops can be carefully removed with P10 micropipette tip.
10. Dissolve RNA in 50 µl of DEPC-treated water by vortexing or passing solution a few times through a pipette tip.
11. To minimize contamination with genomic DNA, treat total RNA with DNase by adding 50 µl of a mix containing 1 µl of DNase (2 U/µl) and 10 µl of 10x DNase buffer in DEPC-treated water. Vortex and spin down.
12. Incubate samples at 37 °C in a water bath or a heating block for 30 to 40 min. After incubation, add 100 µl of DEPC-treated water into each sample.
13. To inactivate the enzymatic activity and clean RNA from DNase, add 200 µl of phenol:chloroform:isoamyl alcohol (25:24:1) solution, vortex for 1 min and centrifuge the samples at 10,000 x g for 7 min at 4 °C.
14. Carefully transfer the upper aqueous phase containing RNA into a fresh tube. Add equal volume (200 µl) of chloroform, mix and repeat the centrifugation step from above.
15. Collect carefully the upper phase and precipitate RNA by adding 1/10 volume of 3 M sodium acetate, pH 5.2 prepared in DEPC H_2O and 2.5 volumes of 100% ethanol. Mix thoroughly by vortexing.
   NOTE: Adding 0.5 µl glycogen (20 µg/µl) to a precipitation mix helps to visualize the RNA pellet. To minimize RNA loss, use siliconized, low-binding 1.5 ml microcentrifuge tubes.
16. Precipitate RNA at -20 °C for at least 1 hr.
   NOTE: The incubation might be carried out overnight. Samples can be placed at -80 °C as well.
17. Pellet RNA by centrifugation at 10,000 x g for 30 min at 4 °C. Wash and dry pellet following the description in 7.9.
18. Dissolve RNA in 10-15 µl of DEPC-treated water. Store RNA at -80 °C.
19. Determine quantity and purity of RNA by measuring OD at 230 nm, 260 nm and 280 nm using a spectrophotometer. Calculate RNA concentration by applying the convention that 1 OD at 260 nm equals 40 µg/ml RNA.
   NOTE: The $A_{260/280}$ ratio of "pure" RNA equals 2.0 while an $A_{260/230}$ ratio should be in the range of 2.0-2.2. RNA samples with an $A_{260/280}$ ratio between 1.7 and 2.0 are suitable for downstream applications such as cDNA synthesis. For preparation of mRNA-seq libraries the quality and quantity of RNA should be checked using an automated electrophoresis system. The 28S/18S ratio should be above 1.8.

Representative Results

To demonstrate the potential of the eyFLP-MARCM technique to generate GFP-marked patches of defined genotypes in *Drosophila* EAD, three types of clones were induced: (1) control expressing GFP only, (2) malignant tumors expressing an oncogenic form of the small G-protein Ras (Ras^{V12}) in a background of homozygous loss of a tumor suppressor gene *scribble* ($scrib^{1}$), and (3) overgrowing but non-invasive $ras^{V12}scrib^{1}jnk^{DN}$ clones, where the Jun-N-terminal kinase (JNK) was inactivated by expression of its dominant-negative form (**Figure 4**, **Table 1** for genotypes). It has been shown that the invasiveness of $ras^{V12}scrib^{1}$ clonal tumors requires aberrant activation of JNK signaling and its downstream transcription factors [10,12,23,24]. Moreover, $ras^{V12}scrib^{1}$ tumors promote a strong inflammatory response in the *Drosophila* larva, resulting in infiltration of immune cells (called hemocytes) into the EAD [14,25].

To monitor the levels and spatial distribution of JNK activity within the mosaic tissue and among tumors of distinct genotypes, the established transgenic, JNK-responsive *TRE-DsRed* reporter was employed [26]. Confocal microscopy of the dissected, fixed EAD and EAD/brain complexes revealed marked upregulation of the *TRE-DsRed* reporter activity in the tissues bearing malignant $ras^{V12}scrib^{1}$ tumors (**Figure 4B**). The DsRed signal labeled $ras^{V12}scrib^{1}$ clones in EAD (**Figure 4B**) as well as tumor cells spreading over the brain lobes and invading the VNC (**Figure 4E, 4F**). In contrast, the *TRE-DsRed* reporter activity remained restricted to a string of cells extending from the antennal to the eye part of the control discs (**Figure 4A'**). Blocking JNK signaling resulted in a dramatic decrease of *TRE-DsRed* signal in clonal $ras^{V12}scrib^{1}jnk^{DN}$ tumors (**Figure 4C, 4D**). These data thus provide functional evidence for a requirement of JNK signaling to activate the TRE-dependent transcriptional response in malignant $ras^{V12}scrib^{1}$ tumors. A lineage-specific *hmlΔ-DsRed* reporter, devised for tracing *Drosophila* hemocytes [27,28] showed an accumulation of immune cells in tissues bearing malignant $ras^{V12}scrib^{1}$ tumors (**Figure 5B**). In contrast, only individual hemocytes or a few localized hemocyte patches were detected in control and $ras^{V12}scrib^{1}jnk^{DN}$ mosaic EAD and brain tissues (**Figure 5A, 5C**). Immunostaining with a pan-hemocyte anti-Hemese antibody (H2) [29] confirmed the immune cell identity of *hmlΔ-DsRed* positive cells (**Figure 5D, 5E**). Consistent with published reports [12,23,24], unbiased quantification of tumor invasiveness corroborated a central role of JNK signaling in promoting tumor invasion into the adjacent brain lobes and VNC (**Figure 3C**). Finally, total RNA was isolated from the mosaic EAD. Samples were subjected either to qRT-PCR or analyzed on an automated electrophoresis system for quality and quantity. **Figure 6A** shows significant JNK-dependent upregulation of *matrix metalloproteinase 1* (*mmp1*) transcript in EAD bearing malignant $ras^{V12}scrib^{1}$ clonal tumors, confirming the previously published findings [12,24,30,31]. Assessment of total RNA using an automated electrophoresis system showed that three independent EAD samples had a 28S/18S ratio above 1.8 (**Figure 6B**). However, EAD 2 RNA was partially degraded, reflected by a smear on the gel (**Figure 6C**). In contrast, EAD 3 sample had a low concentration. Multiple bands of higher molecular weight on gel image (**Figure 6B**) and small peaks on the electropherogram (**Figure 6C**), also suggested DNA contamination. Thus, only EAD 1 sample would be suitable for a preparation of mRNA-seq library.

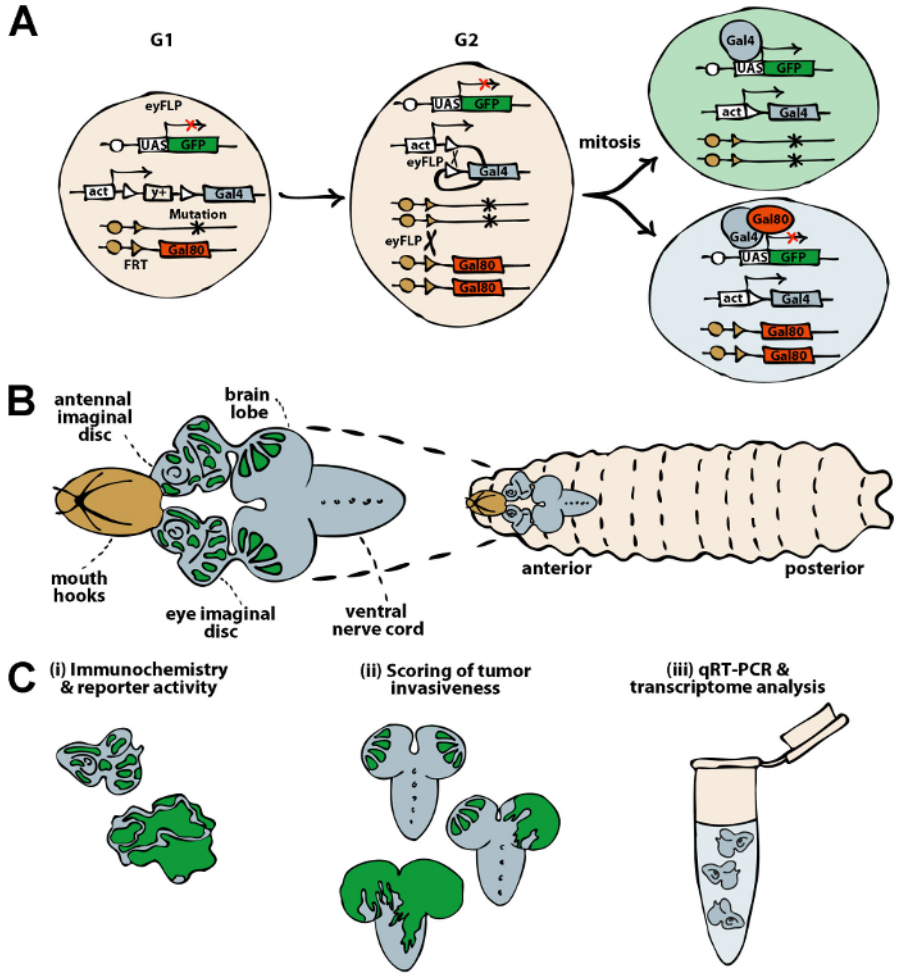

Figure 1: Schematics of the MARCM system for generation of genetic mosaics in the *Drosophila* EAD and downstream applications. (**A**) The MARCM system enables generation of clonal patches with defined genetic lesions in an otherwise wild type (heterozygous) context. The expression of FLP under the control of a tissue specific promoter (*e.g., eyeless*) catalyzes recombination between the two FRT elements flanking the STOP cassette marked with a *yellow (y)* gene (*act>y*$^{+}$*>Gal4*). Upon removal of the STOP cassette, the ubiquitously expressed Gal4 transcriptional activator (*act-Gal4*) can drive expression of any UAS-based transgene such as *UAS-GFP* (also *UAS-ras*^{V12}). In a parental cell, however, the Gal4 activity is blocked by a Gal80 repressor whose expression is controlled by a *tubulin* promoter (*tub-Gal80*). In the G2 phase of the cell cycle, FLP mediates the exchange of the non-sister chromatids between the homologous chromosomes distal to the FRT sites. The segregation of the recombinant chromosomes during mitosis will give rise to two daughter cells, one being homozygous mutant for a particular genomic locus (*e.g.*, *scrib*^{1}) while the other will carry two wild type alleles. Loss of Gal80 in the homozygous mutant cells will permit expression of GFP. In contrast, a wild type sister stays GFP-negative. (**B**) A schematic drawing of a third instar larva depicts the EAD pair connected anteriorly to the mouth hooks and posteriorly to the brain via optic stalks. The eyFLP-MARCM system induces GFP-marked clones within the EAD and the neuroepithelium of the brain lobes. (**C**) Dissected EAD and brains can be subjected to diverse downstream applications including immunochemistry and detection of transgenic reporter activity (*i*), quantification of tumor invasiveness (*ii*) and transcriptome profiling using a candidate (qRT-PCR) or an unbiased approach (mRNA-seq) (*iii*). Please click here to view a larger version of this figure.

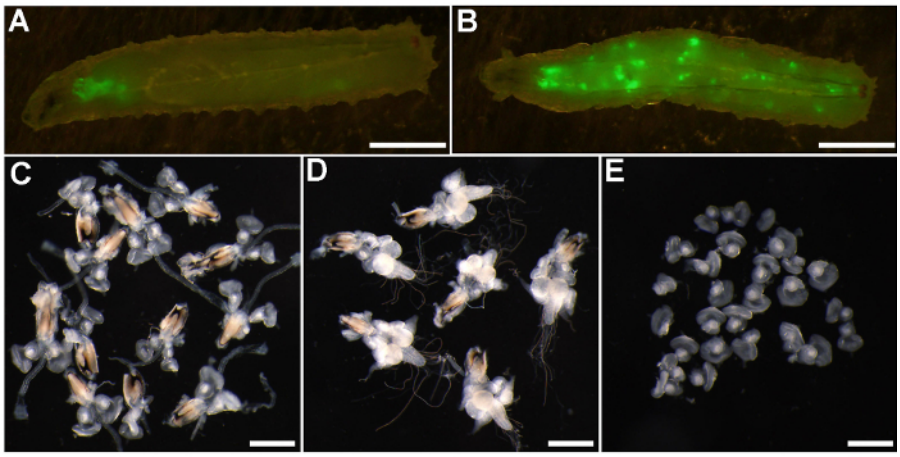

Figure 2: Sorting of third instar larvae and representative examples of EAD and EAD/brain complexes used for different downstream applications. (**A-B**) Fluorescent micrographs of the third instar larvae bearing control GFP-labeled clones induced with the eyFLP-MARCM 82B Green tester. (**A**) Representative control larva with clones restricted to the EAD and brain lobes. (**B**) An example of a "leopard larva" carrying GFP-positive clones in various tissues throughout the body. (**C**) Brightfield images of dissected EAD and (**D**) EAD/brain complexes attached to the mouth hooks, and (**E**) EAD cleaned from all extraneous tissue including mouth hooks. Scale bars = 2 mm (A-B) and 500 µm (C-E). Please click here to view a larger version of this figure.

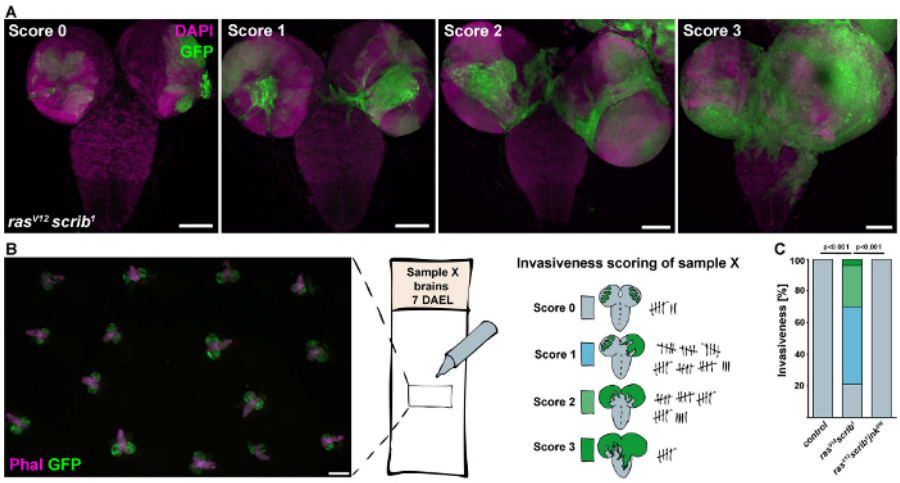

Figure 3: Quantification of tumor invasiveness. (**A**) Fluorescent confocal images of brains dissected from *ras*^{V12} scrib^{1} larvae (7 days AEL) represent the real examples of the four different grades of tumor invasiveness ranging from non-invasive (Score 0), one brain lobe invaded (Score 1), both brain lobes invaded (Score 2) to a strong tumor invasion with clonal tissue covering both brain lobes and entering the VNC (Score 3). Images are projections of multiple confocal sections and examples for Score 2 and 3 are stitched from 2 x 2 confocal images. Scale bars = 100 µm. (**B**) An example of an anonymized microscope slide with fixed brains used for unbiased scoring under a fluorescent stereomicroscope. Scored brains are marked with a pen to prevent duplicate registration. Scale bar = 500 µm (**C**) Compared to highly invasive *ras*^{V12}*scrib*^{1} tumors, inhibition of JNK signaling (*ras*^{V12}*scrib*^{1}*jnk*^{DN}) eliminated invasion of clonal cells. Please click here to view a larger version of this figure.

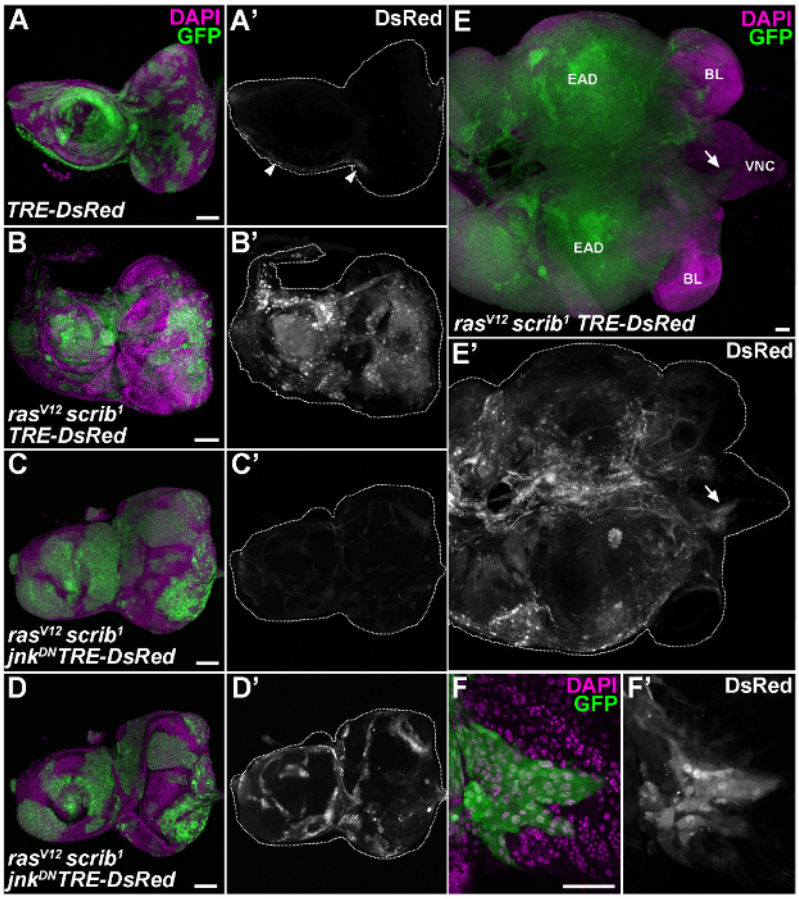

Figure 4: Activation of the transcriptional *TRE-DsRed* reporter in malignant *ras^{V12}scrib^{1}* clonal tumors is JNK-dependent. (**A**) In control EAD (6 days AEL), the JNK-sensitive *TRE-DsRed* reporter labeled a narrow stripe of cells running from antennal to eye part (arrowheads). (**B**) The activity of the *TRE-DsRed* reporter was markedly enhanced in *ras^{V12}scrib^{1}* GFP-positive clones compared to the surrounding non-clonal EAD epithelium. (**C**) Inhibition of JNK activity resulted in a clear reduction of DsRed signal intensity in *ras^{V12}scrib^{1}jnk^{DN}* clones. (**D**) Further enhancement of the DsRed signal revealed non-autonomous activation of JNK signaling in cells surrounding the *ras^{V12}scrib^{1}jnk^{DN}* clones. (**E**) On day 8 AEL, *ras^{V12}scrib^{1}* cells overgrew the entire EAD and spread over the brain lobes to the VNC (arrow). (**F**) The clonal cells invading the VNC (close-up of the region marked by the arrow in E) were enriched for the DsRed signal. (A-C) Show projections of multiple confocal sections, (E) is stitched from 3x3 confocal images and (D, F) represent single section. Scale bars = 50 µm. EAD, eye/antennal disc; BL, brain lobe; VNC, ventral nerve cord. Please click here to view a larger version of this figure.

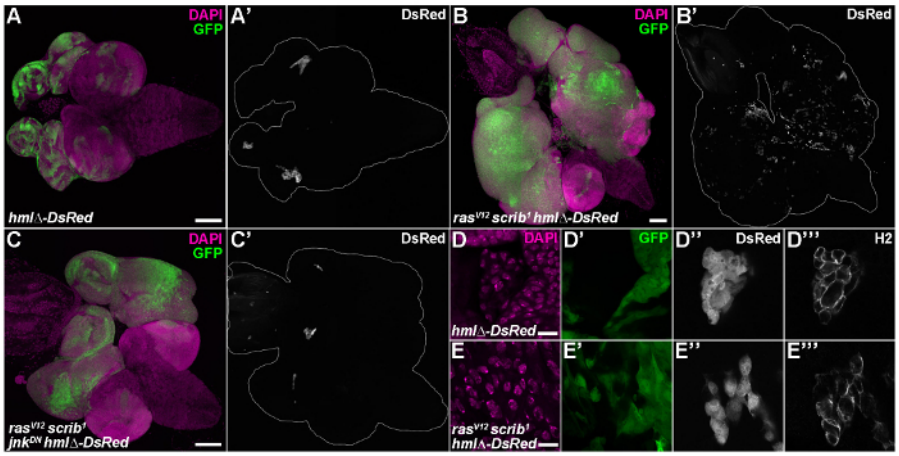

Figure 5: Lineage-specific *hmlΔ-DsRed* transgenic reporter reveals enrichment of *ras^{V12}scrib^{1}* tumor-associated hemocytes. (**A**) In control EAD, *hmlΔ-DsRed* reporter-labeled hemocyte clusters are trapped in the indentations of the eye and antennal epithelium. (**B**) EAD and brain tissue comprised of *ras^{V12}scrib^{1}* GFP-marked tumors showed an increased number of hemocytes scattered all over the clonal tissue. (**C**) The number of associated hemocytes dramatically decreased upon inhibition of JNK signaling in *ras^{V12}scrib^{1}jnk^{DN}* mosaic tissue. (**D-E**) *HmlΔ-DsRed* positive hemocytes were also labeled with an H2-antibody that detects the pan-hemocyte marker Hemese. (A-C) Show projections of multiple confocal sections, (A) is stitched from 2 x 2 and (B-C) are stitched from 3 x 3 confocal images. (D-E) Represent single sections. Scale bars = 100 µm (A-C) and 10 µm (D-E). Please click here to view a larger version of this figure.

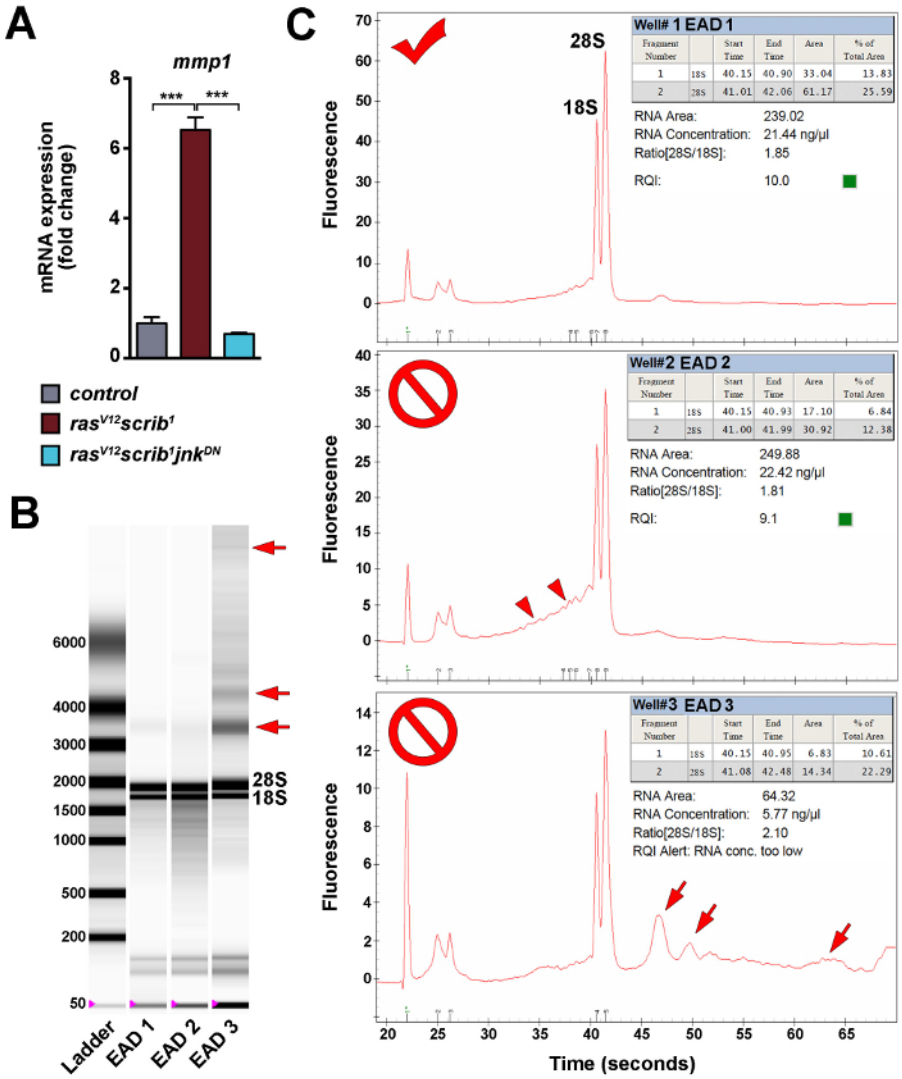

Figure 6: Evaluation of quantity and quality of total RNA isolated from dissected EAD. (**A**) A representative example of qRT-PCR results using four biological replicates for each genotype. *Mmp1* transcript levels were normalized to *rp49*. Fold changes in gene expression were calculated using the relative standard curve method [32]. Data are mean values ± s.e.m.; ***P <0.001 using Student's unpaired two-tailed t-test with unequal variance. (**B, C**) Assessment of total RNA quality and quantity using an automated electrophoresis system. The virtual gel image (**B**) shows the two prominent bands of the 18S and 28S rRNAs that correspond to the well-defined peaks on electropherograms (**C**). DNA contamination and RNA degradation are reflected by a smear (arrowheads) and extranumerary bands and peaks (arrows). Please click here to view a larger version of this figure.

Fly Strains	Source/Comments
eyFLP1; act>y^{+}>Gal4, UAS-GFP; FRT82B, tub-Gal80	eyFLP-MARCM 82B Green Tester [11]
w; UAS-ras^{V12}; FRT82B scrib^{1}/TM6B	[12]
w; UAS-ras^{V12}; UAS-jnk^{DN} FRT82B scrib^{1}/TM6B	[12]
w; hmlΔ-DsRed; FRT82B	this study, *w; hmlΔ-DsRed* from Katja Brückner [28]
w; UAS-ras^{V12} hmlΔ-DsRed; FRT82B scrib^{1}/TM6B	this study
w; UAS-ras^{V12} hmlΔ-DsRed; UAS-jnk^{DN} FRT82B scrib^{1}/TM6B	this study
w; TRE-DsRed; FRT82B	this study, *w; TRE-DsRed* from Dirk Bohmann [26]
w; UAS-ras^{V12} TRE-DsRed; FRT82B scrib^{1}/TM6B	this study
w; UAS-ras^{V12} TRE-DsRed; UAS-jnk^{DN} FRT82B scrib^{1}/TM6B	this study

Table 1: Summary of *Drosophila* lines used in this study.

Discussion

The techniques to generate genetic mosaics in *Drosophila* are among the most sophisticated tools for analyzing and manipulating gene function [33]. The eyFLP-MARCM system has proven powerful and robust as it allows the induction of visually marked, genetically defined clones in a spatially restricted manner, *i.e.*, in tissues where the *eyeless* enhancer is active [9,18]. This is particularly important when multiple genetic lesions are combined in the same cells. While these highly aberrant patches permit larval development when restricted to the EAD and brain neuroepithelia, they can cause lethality when scattered throughout the larval body as in the case of heat shock-controlled FLP (hsFLP) clones. Significantly, induction of clones in the fly EAD epithelium in which activated oncogenes combine with loss of tumor suppressors recapitulates the emergence and progression of solid epithelial tumors in some human cancers. However, the system also has its limitations that will be briefly discussed. Given that insects have an open circulatory system, true metastases as observed in human cancers do not occur. Therefore the complex process of metastatic dissemination cannot be faithfully modeled in *Drosophila*. Nevertheless, EAD tumors such as the *ras^{V12}scrib^{1}* clones do display malignant properties as they break down the basal membrane surrounding the EAD and invade the adjacent brain [11,12,31]. The degree of tumor aggressiveness can be quantified and compared among different genotypes as described in this study. It is also important to note that the presence of specific genetic lesions in mosaic EAD might affect developmental timing and duration of larval growth. Staging of larvae will determine whether analysis of mosaic tissue will be done using animals of the same chronological or developmental stage. Performing a pilot experiment to assess the impact of a new EAD clonal genotype on developmental timing is desirable.

There are technical limitations as well. First, the number of different clonal genotypes that can be built with the eyFLP-MARCM tool is great but not infinite. For instance, combining two mutant alleles that reside on different chromosomes is hindered by low efficiency of recombination on both chromosomes simultaneously, and genes located on the small fourth chromosome are generally inaccessible. Gene knockdown using transgenic RNAi is an alternate solution. However, it is important to realize that transgenes are not expressed immediately upon mitotic recombination — not until the Gal80 repressor is degraded. The activity of the Gal4/UAS expression system can be enhanced by growing larvae at 29 °C. It is, however, important to keep in mind that elevated temperature affects various developmental, physiological and molecular parameters including growth rate, developmental timing, metabolism and gene expression [34-37]. Thus, adaptations to the provided protocols such as staging of the larvae or number of dissected EAD for transcriptome profiling would be necessary.

The eyFLP-MARCM testers are not among the healthiest strains. The multiple transgenes in one genome compromise fly fitness and fecundity. These stocks require extra attention to be maintained and expanded for large collections of virgin females. As documented in this study, the MARCM 82B Green tester line [11], although viable when homozygous, is genetically unstable. This is obvious from the spontaneous appearance of "leopard larvae" that display ectopic, GFP-labeled clones within various polyploid tissues including the intestine, tracheae, fat body, and larval epidermis. This phenomenon occurs in all crosses independent of the paternal genotype. We presume that the ectopic GFP patches result from uncontrolled, stochastic recombination between the two FRT sites in the FLP-out cassette, causing removal of the *yellow^{+}* marker and the "STOP cassette". In the polyploid tissues, the *tubulin* promoter-driven Gal80 repressor might be insufficient to block the Gal4 activity. The presence of genetically modified cells in tissues other than the EAD and brain could elicit systemic signals that might affect behavior of the experimental clones. These "leopard larvae" should therefore be excluded from analyses. Moreover, we routinely re-establish the MARCM 82B Green tester from single male-female crosses.

Despite the pitfalls mentioned above, the applications of the eyFLP-MARCM system to study gene functions and the interactions between clonal tumors and their environment are manifold. Introduction of the Gal4/UAS-independent binary expression systems such as LexA/LexOp [38] or drug controllable QF/QUAS/QS [39,40] would provide a fine control over transgene expression and/or simultaneous labeling and manipulation of different cell populations including clonal, non-clonal epithelial cells and hemocytes. Such mosaic tissues could be again processed according to protocols described here.

The method for dissection of mosaic EAD and EAD/brain complexes from the third instar larvae (Protocol section 3) can be applied to earlier developmental stages as well. Importantly, the protocol for EAD/brain complexes permits recovery of the wing, haltere and leg imaginal discs. Should these be used for RNA isolation (Protocol sections 3.3.2 and 7), the disc of interest should be cleaned from extraneous tissue and processed similarly to EAD. Given their smaller size, the number of haltere and leg discs collected should be increased to acquire sufficient amount of RNA.

The protocol for extraction of total RNA from EAD (Protocol section 7) is based on RNA lysis reagent available from different commercial vendors (see List of Materials/Equipment). The overall success of the procedure mainly depends on: (*i*) having sufficient number of larvae, (*ii*) being quick and precise while dissecting, and (*iii*) keeping samples free from RNases. Keeping the work space and instruments clean, wearing gloves, using RNase-free plastic ware and solutions, and keeping samples on ice all reduce RNA degradation. To prevent contamination of RNA with any genomic DNA that might not be completely removed by the DNase treatment (Protocol section 7.11), it is critical to avoid interphase when collecting the aqueous phase for the first time (Protocol section 7.6). Both DNA contamination and RNA degradation can be revealed by running samples on an automated electrophoresis system (**Figure 6B, 6C**). The RNA isolation protocol has a broader application. It has been successfully used for RNA extraction from whole larvae at different developmental stages, from adults, and various larval organs. The obtained RNA was suitable for both qRT-PCR and genome-wide transcriptome analysis by mRNA-seq [20,24,41,42]. Compared to qRT-PCR that quantifies tens of selected mRNAs at most, unbiased mRNA sequencing permits genome-wide expression analyses. Thus, one can compare entire transcriptome signatures of tumors induced by specific genetic lesions at distinct stages of tumorigenesis [24]. It is important to keep in mind that RNA comes from the entire discs, so that results will not only reflect changes in the clones but also in the surrounding, non-clonal tissue. Performing fluorescent activate cell sorting (FACS) on dissociated mosaic EAD by adapting available protocols [43,44] could be applied to determine transcriptional signature of specific cellular populations, *e.g.*, clonal (GFP^+) and non-clonal (GFP^-) cells.

The fixation and immunostaining protocol described here is suited for simultaneous visualization of proteins of interest with specific antibodies and activity of transgenic reporters. Both the GFP signal marking clonal cells and DsRed fluorescence produced by either of the two transgenic reporters used in this study are preserved throughout fixation and immunostaining and can be directly visualized by confocal microscopy. However, antibodies against the fluorescent proteins can amplify the signal intensity. Similarly, use of an anti-β-galactosidase antibody will facilitate detection of transgenic reporters based on the bacterial *lacZ* gene. Relative reporter activities can be assessed by measuring the relative pixel intensities of clones versus non-clonal tissue using image analysis software (*e.g.,* FiJi, ImageJ). When comparing reporter activity among different clonal genotypes, the image acquisition settings must be kept constant (Protocol section 5 and references [21,22]). Although the protocol works well with many different antibodies, it may be necessary to optimize recommended antibody concentrations. Alterations might also be required in fixation time, type and concentration of detergent (Triton X-100, Tween-20, Saponin) and fixative (8% PFA, 4% formaldehyde, EtOH).

Unlike the protocols discussed above, quantification of tumor invasiveness is limited to the third instar larval stage and the EAD/brain complex. Nevertheless, its overall rationale can apply to any quantitative studies where cognitive bias needs to be avoided. The method requires thoroughness. As tumor malignancy increases in time, it is essential to compare larvae of the same age (*e.g.,* 7 or 8 days after egg laying). With time a clonal tumor can overgrow massively, yet the tumor cells may remain within the EAD. The step in which brains are separated from the EAD (Protocol section 4.4.1) is therefore critical to avoid false-positive invasiveness counts. Mounting of brains with the attached EAD will flatten the tissues, causing the overgrown EAD to cover the brain structures and thus prevent any quantification. Ideally, one would like to capture the invasive process directly in the living larva. Transgenic reporters to visualize the involved cell populations and tissues are available and could be combined with the eyFLP-MARCM system. Unfortunately, the invasive process takes several hours to days, a time frame that is incompatible with keeping the larvae alive while still.

Disclosures

The authors declare that they have no conflict of interest.

Acknowledgements

We thank the Bloomington Stock Center (Bloomington, USA), Dirk Bohmann, Katja Brückner and Istvan Ando for fly stocks, and antibodies. We thank Marek Jindra and Colin Donohoe for comments on the manuscript. This work was supported by the Sofja Kovalevskaja Award to M.U. from the Alexander von Humboldt Foundation and DFG project UH243/1-1 to M.U. from the German Research Foundation.

References

1. Miles, W. O., Dyson, N. J., & Walker, J. A. Modeling tumor invasion and metastasis in Drosophila. *Dis Model Mech.* **4** (6), 753-761 (2011).
2. Stefanatos, R. K. A., & Vidal, M. Tumor invasion and metastasis in Drosophila: a bold past, a bright future. *J Genet Genomics.* **38** (10), 431-438 (2011).
3. Patel, P. H., & Edgar, B. A. Tissue design: How Drosophila tumors remodel their neighborhood. *Semin Cell Dev Biol.* **28**, 86-95 (2014).
4. Gonzalez, C. Drosophila melanogaster: a model and a tool to investigate malignancy and identify new therapeutics. *Nat Rev Cancer.* **13** (3), 172-183 (2013).
5. Lee, T., & Luo, L. Mosaic analysis with a repressible cell marker (MARCM) for Drosophila neural development. *Trends Neurosci.* **24** (5), 251-254 (2001).
6. Xu, T., & Rubin, G. M. Analysis of genetic mosaics in developing and adult Drosophila tissues. *Development.* **117** (4), 1223-1237 (1993).
7. Struhl, G., & Basler, K. Organizing activity of wingless protein in Drosophila. *Cell.* **72** (4), 527-540 (1993).
8. Brand, A. H., & Perrimon, N. Targeted gene expression as a means of altering cell fates and generating dominant phenotypes. *Development.* **118** (2), 401-415 (1993).
9. Wu, J. S., & Luo, L. A protocol for mosaic analysis with a repressible cell marker (MARCM) in Drosophila. *Nat Protoc.* **1** (6), 2583-2589 (2006).
10. Brumby, A. M., & Richardson, H. E. scribble mutants cooperate with oncogenic Ras or Notch to cause neoplastic overgrowth in Drosophila. *EMBO J.* **22** (21), 5769-5779 (2003).
11. Pagliarini, R. A., & Xu, T. A genetic screen in Drosophila for metastatic behavior. *Science (New York, NY).* **302** (5648), 1227-1231 (2003).
12. Uhlirova, M., & Bohmann, D. JNK- and Fos-regulated Mmp1 expression cooperates with Ras to induce invasive tumors in Drosophila. *EMBO J.* **25** (22), 5294-5304 (2006).

13. Turkel, N., *et al.* The BTB-zinc finger transcription factor abrupt acts as an epithelial oncogene in Drosophila melanogaster through maintaining a progenitor-like cell state. *PLoS Genet.* **9** (7), e1003627 (2013).
14. Cordero, J. B., *et al.* Oncogenic Ras Diverts a Host TNF Tumor Suppressor Activity into Tumor Promoter. *Dev Cell.* **18** (6), 999-1011 (2010).
15. Khoo, P., Allan, K., Willoughby, L., Brumby, A. M., & Richardson, H. E. In Drosophila, RhoGEF2 cooperates with activated Ras in tumorigenesis through a pathway involving Rho1-Rok-Myosin-II and JNK signalling. *Dis Model Mech.* **6**, 661-678 (2013).
16. Jiang, Y., Scott, K. L., Kwak, S.-J., Chen, R., & Mardon, G. Sds22/PP1 links epithelial integrity and tumor suppression via regulation of myosin II and JNK signaling. *Oncogene.* **30** (29), 3248-3260 (2011).
17. Figueroa-Clarevega, A., & Bilder, D. Malignant Drosophila Tumors Interrupt Insulin Signaling to Induce Cachexia-like Wasting. *Dev Cell.* **33** (1), 47-55 (2015).
18. Newsome, T. P., Asling, B., & Dickson, B. J. Analysis of Drosophila photoreceptor axon guidance in eye-specific mosaics. *Development.* **127** (4), 851-860 (2000).
19. Quiring, R., Walldorf, U., Kloter, U., & Gehring, W. J. Homology of the eyeless gene of Drosophila to the Small eye gene in mice and Aniridia in humans. *Science.* **265** (5173), 785-789 (1994).
20. Külshammer, E., & Uhlirova, M. The actin cross-linker Filamin/Cheerio mediates tumor malignancy downstream of JNK signaling. *J Cell Sci.* **126** (Pt 4), 927-938 (2013).
21. North, A. J. Seeing is believing? A beginners' guide to practical pitfalls in image acquisition. *J Cell Biol.* **172** (1), 9-18 (2006).
22. Waters, J. C. Accuracy and precision in quantitative fluorescence microscopy. *J Cell Biol.* **185** (7), 1135-1148 (2009).
23. Igaki, T., Pagliarini, R. A., & Xu, T. Loss of cell polarity drives tumor growth and invasion through JNK activation in Drosophila. *Curr Biol.* **16** (11), 1139-1146 (2006).
24. Külshammer, E., *et al.* Interplay among Drosophila transcription factors Ets21c, Fos and Ftz-F1 drives JNK-mediated tumor malignancy. *Dis Model Mech.* **8** (10), 1279-1293 (2015).
25. Pastor-Pareja, J. C., Wu, M., & Xu, T. An innate immune response of blood cells to tumors and tissue damage in Drosophila. *Dis Model Mech.* **1** (2-3), 144-154 (2008).
26. Chatterjee, N., & Bohmann, D. A versatile ΦC31 based reporter system for measuring AP-1 and Nrf2 signaling in Drosophila and in tissue culture. *PloS One.* **7** (4), e34063 (2012).
27. Petraki, S., Alexander, B., & Brückner, K. Assaying Blood Cell Populations of the Drosophila melanogaster Larva. *J Vis Exp.* (105) (2015).
28. Makhijani, K., Alexander, B., Tanaka, T., Rulifson, E., & Bruckner, K. The peripheral nervous system supports blood cell homing and survival in the Drosophila larva. *Development.* **138** (24), 5379-5391 (2011).
29. Kurucz, E., *et al.* Hemese, a hemocyte-specific transmembrane protein, affects the cellular immune response in Drosophila. *Proc Natl Acad Sci USA.* **100** (5), 2622-2627 (2003).
30. Andersen, D. S., *et al.* The Drosophila TNF receptor Grindelwald couples loss of cell polarity and neoplastic growth. *Nature.* **522** (7557), 482-486 (2015).
31. Srivastava, A., Pastor-Pareja, J. C., Igaki, T., Pagliarini, R., & Xu, T. Basement membrane remodeling is essential for Drosophila disc eversion and tumor invasion. *Proc Natl Acad Sci USA.* **104** (8), 2721-2726 (2007).
32. Larionov, A., Krause, A., & Miller, W. A standard curve based method for relative real time PCR data processing. *BMC Bioinformatics.* **6** (1), 62 (2005).
33. Blair, S. S. Genetic mosaic techniques for studying Drosophila development. *Development.* **130** (21), 5065-5072 (2003).
34. Mirth, C. K., & Shingleton, A. W. Integrating body and organ size in Drosophila: recent advances and outstanding problems. *Front Endocrinol.* **3**, 49 (2012).
35. French, V., Feast, M., & Partridge, L. Body size and cell size in Drosophila: the developmental response to temperature. *J Insect Physiol.* **44** (11), 1081-1089 (1998).
36. Ashburner, M., & Bonner, J. J. The induction of gene activity in drosophila by heat shock. *Cell.* **17** (2), 241-254 (1979).
37. Frazier, M. R., Woods, H. A., & Harrison, J. F. Interactive effects of rearing temperature and oxygen on the development of Drosophila melanogaster. *Physiol Biochem Zool.* **74** (5), 641-650 (2001).
38. Lai, S.-L., & Lee, T. Genetic mosaic with dual binary transcriptional systems in Drosophila. *Nat Neurosci.* **9** (5), 703-709 (2006).
39. Potter, C. J., Tasic, B., Russler, E. V., Liang, L., & Luo, L. The Q system: a repressible binary system for transgene expression, lineage tracing, and mosaic analysis. *Cell.* **141** (3), 536-548 (2010).
40. del Valle Rodrìguez, A., Didiano, D., & Desplan, C. Power tools for gene expression and clonal analysis in Drosophila. *Nature Methods*. **9** (1), 47-55 (2011).
41. Rynes, J., *et al.* Activating Transcription Factor 3 Regulates Immune and Metabolic Homeostasis. *Mol Cell Biol.* **32** (19), 3949-3962 (2012).
42. Claudius, A.-K., Romani, P., Lamkemeyer, T., Jindra, M., & Uhlirova, M. Unexpected role of the steroid-deficiency protein ecdysoneless in pre-mRNA splicing. *PLoS Genet.* **10** (4), e1004287 (2014).
43. Basu, S., Campbell, H. M., Dittel, B. N., & Ray, A. Purification of Specific Cell Population by Fluorescence Activated Cell Sorting (FACS). *J Vis Exp.* (41) (2010).
44. Tauc, H. M., Tasdogan, A., & Pandur, P. Isolating intestinal stem cells from adult Drosophila midguts by FACS to study stem cell behavior during aging. *J Vis Exp.* (94) (2014).

